8-16-2023

Performance analysis of wireless compressed-image transmission over DST-based OFDMA systems

Nagi H. Al-Ashwal

Khaled A. M. Al Soufy

Faisal S. Al-Kamali

Mohamed Swillam

EURASIP Journal on Wireless Communications and Networking

RESEARCH Open Access

Performance analysis of wireless compressed-image transmission over DST-based OFDMA systems

Nagi H. Al-Ashwal[1,2], Khaled A. M. Al Soufy[1,2*], Faisal S. Al-Kamali[2,3] and Mohamed Swillam[1]

*Correspondence: kalsoufi@gmail.com

[1] Department of Physics, American University in Cairo, New Cairo 11835, Egypt
[2] Department of Electrical Engineering, Ibb University, Ibb City, Yemen
[3] School of Electrical Engineering and Computer Science, Ottawa University, Ottawa, ON K1N 6N5, Canada

Abstract

Multimedia data, like images, consumes significant bandwidth when transmitted over wireless systems. Therefore, compressing transmitted images becomes crucial to reduce the required bandwidth and improve energy efficiency. This work aims to analyze the performance of transmitting wireless compressed images over a recent Discrete Sine Transform (DST)-Based Orthogonal Frequency Division Multiple Access (DST-OFDMA) system. It investigates the effectiveness of several image compression methods by determining the minimum Signal-to-Noise Ratio (SNR) required for each method to achieve error-free image recovery at the receiver. This work considers different modulation schemes including 16QAM and QPSK, as well as different subcarrier mapping schemes (localized and interleaved) over vehicular A, SUI3, and uniform channels. Nine standard compression methods are used for analyzing the performance of the DST-OFDMA system and compared it with that of the conventional Discrete Fourier Transform (DFT)-based OFDMA (DFT-OFDMA) system. The results show that the performance of DST-OFDMA outperforms that of DFT-OFDMA, especially when QPSK modulation is used. Simulation results demonstrate that the interleaved DST-OFDMA (DST-IOFDMA) system, employing the SPIHT_3D compression method and QPSK modulation (over the SUI3 channel model), achieves the lowest SNR value required for compressed image recovery, approximately 18 dB. This indicates that the SPIHT_3D compression method exhibits lower power consumption compared to other methods as well as high bandwidth efficiency.

Keywords: DFT and DST basis functions, OFDMA system, Image compression

1 Introduction

Orthogonal frequency division multiple access (OFDMA) system is one of the most common multiple access techniques used in the uplink of modern wireless communication standards due to its ability to support high-speed data transfer, low-latency communication, and a large number of users [1]. It has been adopted as the standard for many wireless communication systems, including Wi-Fi, long-term evolution (LTE) standard, and currently 5th generation standard. It can efficiently transmit many forms of multimedia communication of data compared to other existing traditional communication systems. Image transmission via wireless communication plays a crucial role in

various everyday applications. It enables instantly sharing and receiving visual information across different devices and platforms. From social media platforms and messaging apps to video conferencing and remote surveillance systems, wireless image transmission enhances communication, facilitates remote collaborations, and enables real-time visual interactions [2]. OFDMA system has been widely used by various wireless image transmission standards. The image transmission performance over OFDMA was implemented and investigated with various basis functions in [3, 4]. But there are few works have been done in the transmission of compressed images over wireless communication systems.

Image compression and transmission over wireless communication systems is a complex and challenging task that requires careful consideration of various factors such as image quality, bandwidth, and transmission reliability. The compressed-image transmission over wireless communication systems has been studied by many researchers, for example, see [5–12]. In [13], the wireless transmission of the compressed image was evaluated over the OFDMA system with only discrete Fourier transform (DFT) as a basis function. On the other hand, the existing literature has not explored the wireless transmission of compressed images as an application over the OFDMA system using discrete sine transform (DST) as a basis function, which is the primary objective of this paper. This motivated us to do this research work and investigate the performance of wireless transmission of compressed images utilizing the DST in OFDMA systems. This paper aims to analyze the transmission of compressed images over DST-OFDMA for different compression methods, various subcarrier mapping schemes, including interleaved and localized subcarriers mapping, and different modulation schemes, such as QPSK and 16QAM, over SUI3, vehicular A, and uniform channels. Specifically, it aims to determine the compressed method that requires low power consumption by determining the minimum SNR necessary to achieve the accurate reconstruction of compressed images. Whereas in [14], the authors discussed the DST-OFDMA system to allow the application of efficient transmission of non-compressed data over wireless channels. DST-OFDMA is a communication system that combines DST and OFDMA in which the DST is used as a basis function, while OFDMA is used to divide the available bandwidth into multiple subcarriers, allowing multiple users to transmit simultaneously without interfering with each other. The use of DST enables efficient compression of data, while OFDMA enables multiple users to transmit their data simultaneously without interference [15]. This makes DST-OFDMA particularly useful for high-speed wireless communication applications, such as video streaming and real-time data transfer.

The contribution of this paper can be summarized as follows:

1. This paper is the first one to study and analyze the performance of compressed image transmission over the DST-OFDMA system and compare the obtained results with that over the conventional DFT-OFDMA system. Nine compression methods are evaluated over three different scenarios for different mapping systems: DFT-interleaved OFDMA (IOFDMA), DFT-localized OFDMA (LOFDMA), DST-IOFDMA, and DST-LOFDMA.

a. In the first scenario, 16QAM and QPSK modulations were used over the vehicular A channel model.
b. In the second scenario, 16QAM and QPSK modulations were used over the SUI3 channel model.
c. In the third scenario, 16QAM and QPSK modulations were used over the uniform channel model.

2. To assess the performance in each scenario, we will calculate the minimum required SNR for successfully recovering the transmitted compressed image. This comparison metric will help identify the system with lower power consumption in each scenario. The power consumption of the compression method with a low SNR will be lower compared to the compression method with a high SNR.
3. Simulation results are performed using MATLAB to investigate and find the best compression method that requires a low power consumption to detect the compressed image without error at different scenarios by determining the required minimum SNR.

In future research, we can improve bandwidth utilization and make our systems more energy efficient. This can be done by combining different techniques such as reconfigurable intelligent surface (RIS) [16], rate-splitting multiple access (RSMA) [17], and energy-efficient beamforming [18]. This paper focused on a single-input single-output (SISO) scenario with a convolutional code and QPSK or 16QAM modulation, similar to 4G systems, at a frequency of 2 MHz. Expanding this research to include more advanced techniques such as 256 QAM modulation, LDPC code, and multiple-input multiple-output (MIMO) systems operating in the millimeter wave frequency band, as seen in 5G networks, would be of interest. Additionally, incorporating hybrid precoding and combining techniques, as demonstrated in reference [19], could further enhance the study.

The rest of this paper is organized as follows. Section 2 introduces the DST-OFDMA system model. Section 3 discusses various image compression methods. Section 4 presents and discusses the simulation results for the DST-OFDMA system using several image compression methods. Finally, Sect. 5 draws conclusions based on the simulation results.

2 OFDMA system model

2.1 DST-OFDMA system

The OFDMA system is an extension of the OFDM system designed to support multiple users. In an OFDMA system, each user is assigned specific subcarriers during specific time for communication. To simplify the allocation process and minimize overhead, subcarriers are typically assigned in contiguous groups. However, a key challenge in OFDMA systems is synchronizing the uplink transmission to prevent interference between users. In this section, we explore the use of DST as the basis function in the OFDMA system, resulting in the DST-OFDMA system model. The DST offers several advantages over the DFT. Unlike the DFT, the DST utilizes only real arithmetic

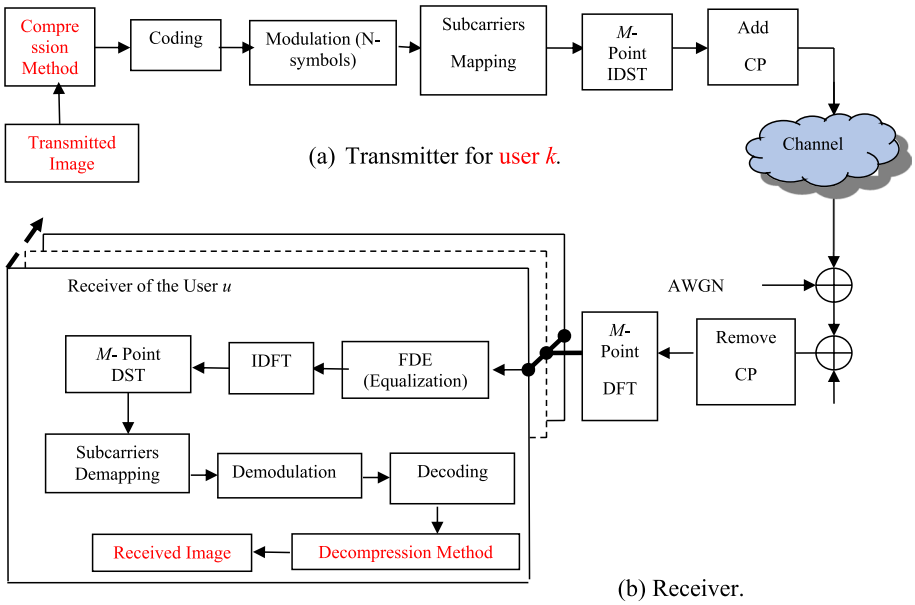

Fig. 1 Structure of the uplink DST-OFDMA system. The figure shows the structure of the uplink for a discrete sine transform OFDMA system, which is divided into three parts: the transmitter site, the channel, and the receiver site

operations instead of complex arithmetic. This reduces the complexity of signal processing and minimizes in-phase/quadrature imbalance issues.

Figure 1 illustrates the structure of the uplink DST-OFDMA system. The system consists of K users and one base station. A total of M subcarriers are available, and each user is allocated a subset of N subcarriers for their uplink transmission. It is assumed that all users have an equal number of subcarriers for simplicity. The transmitter in the OFDMA system utilizes two subcarrier mapping schemes, the interleaved and the localized.

At the transmitter side in Fig. 1, the received image is first compressed using one of the compression methods and then encoded using a convolutional code. Then, the encoded data is transformed into a multilevel sequence of complex numbers using various modulation formats such as QPS an 16QAM. These modulated symbols are then grouped into blocks, each containing N symbols, and subjected to either interleaved or localized subcarrier mapping techniques. Next, an M-point Inverse DST (IDST) process is applied. Finally, to facilitate frequency domain equalization at the receiver side and mitigate inter-block interference, a cyclic prefix (CP) is added. The CP ensures that linear convolution is converted into circular convolution. Additionally, the CP helps remove inter-block interference. After adding a CP to the resulting signal, the signal is transmitted through the wireless channel.

In matrix notation, the transmitted signal of the *kth* user ($k = 1,2,\ldots,K$) can be formulated as follows:

$$\widetilde{\mathbf{x}}^{\mathrm{k}} = \mathbf{P}_{\mathrm{add}}\mathbf{S}_{\mathrm{M}}{}^{-1}\mathbf{M}_{\mathrm{T}}^{\mathrm{k}}\mathbf{d}^{\mathrm{k}} \tag{1}$$

where $\mathbf{d}^k$ is an $N \times 1$ vector containing the modulated symbols of the *kth* user. $\boldsymbol{S}_M^{-1}$ represents an $M \times M$ IDST matrix. The matrix $\boldsymbol{M}_T^k$ is an $M \times N$ matrix that describes the subcarriers mapping for the *kth* user. Here, M is equal to $Q.N$, where Q is the maximum number of users that can transmit, simultaneously. $\mathbf{P}_{add}$ represents an $(M+N_C) \times M$ matrix, which adds a CP of length N_C.

For the localized DFT-OFDMA, the entries of $\boldsymbol{M}_T^k$ IS given by [15]:

$$\boldsymbol{M}_T^k = [0_{(k-1)N \times N}; \boldsymbol{I}_N; 0_{(M-kN) \times N}] \tag{2}$$

For the interleaved DFT-OFDMA, the entries of $\boldsymbol{M}_T^k$ IS given by [15]:

$$\boldsymbol{M}_T^k = [0_{(k-1) \times N}; \boldsymbol{u}_1^T; 0_{(Q-k) \times N}; ...; 0_{(k-1) \times N}; \boldsymbol{u}_N^T; 0_{(Q-k) \times N}] \tag{3}$$

where the $\mathbf{I}_N$ and $\mathbf{0}_{Q' \times N}$ matrices denote the $N \times N$ identity matrix, and the $Q' \times N$ all-zero.

matrix, respectively. $\mathbf{u}_l$ (l = 1, 2, ..., N) denotes the unit column vector, of length N, with all zero entries except at l. $\mathbf{P}_{add}$ can be represented as follows [15]:

$$\boldsymbol{P}_{add} = [\boldsymbol{C}, \boldsymbol{I}_M]^T \tag{4}$$

where

$$\boldsymbol{C} = [0_{N_C \times (M-N_C)}, \boldsymbol{I}_{N_C}]^T \tag{5}$$

At the receiver side, after removal the CP, the frequency domain equalization (FDE) is performed and then the DST, the subcarriers demapping, the demodulation and the decoding processes are applied. The received signal after removing the CP can be expressed as

$$\boldsymbol{r} = \sum_{\boldsymbol{k}=1}^{K} \boldsymbol{H}_{\boldsymbol{C}}^k \mathbf{S}_{\mathrm{M}}{}^{-1} \mathbf{M}_{\mathrm{T}}^{\mathrm{k}} \mathbf{d}^{\mathrm{k}} + \boldsymbol{n} \tag{6}$$

where $\boldsymbol{H}_C^k$ represents an $M \times M$ circulant matrix of the multipath channel between the base station and the *kth* user. $\boldsymbol{n}$ is an $M \times 1$ vector describes the additive noise. $\mathbf{H}_C^u$ is given by [15]:

$$\mathbf{H}_C^u = \begin{bmatrix} h^u[0] & 0 & . & 0 & h^u[L-1] & . & h^u[1] \\ . & h^u[0] & . & & . & . & . \\ . & & . & . & & . & h^u[L-1] \\ h^u[L-1] & & & . & . & & 0 \\ 0 & . & & & . & . & . \\ . & . & . & & & . & 0 \\ 0 & . & 0 & h^u[L-1] & . & . & h^u[0] \end{bmatrix} \tag{7}$$

The circulant matrix $\mathbf{H}_C^u$ can be written as:

$$\mathbf{H}_C^u = \mathbf{F}^{-1} \boldsymbol{\Lambda}^u \mathbf{F} \tag{8}$$

where $\mathbf{F}$ and $\mathbf{F}^{-1}$ are the M × M DFT and the M × M IDFT matrices, respectively. $\boldsymbol{\Lambda}^u$ is an $M \times M$ diagonal matrix containing the DFT of the circulant sequence of $\mathbf{H}_C^u$.

After substituting Eq. (8) into Eq. (6) and applying the DFT, we obtain:

$$\mathbf{R} = \sum_{k=1}^{K} \mathbf{\Lambda}^{k} \mathbf{F}_{M} \mathbf{S}_{M}{}^{-1} \mathbf{M}_{T}^{k} \mathbf{d}^{k} + \mathbf{N} \tag{9}$$

where $\mathbf{\Lambda}^{k}$ is an M × M diagonal matrix that contains the DFT of the circulant sequence of the *kth* user. **N** is the DFT of ***n***. After that, the FDE can be performed using the minimum mean square error (MMSE) criteria. This is followed by the IDFT, DST, and subcarrier demapping processes to obtain the estimated modulated symbols, as described mathematically by Eq. (4).

$$\widehat{\mathbf{d}}_{k} = \mathbf{M}_{R}^{k} \mathbf{S}_{M} \mathbf{F}_{M}^{-1} \boldsymbol{W}_{MMSE}{}^{k} \mathbf{R} \tag{4}$$

where $\boldsymbol{W}_{MMSE}{}^{k}$ is the $M \times M$ FDE matrix of the *kth* user based on the MMSE criteria, $\mathbf{F}_{M}^{-1}$ is an $M \times M$ invers DFT matrix, $\mathbf{S}_{M}$ is an $M \times M$ DST matrix, and $\mathbf{M}_{R}^{k}$ is the subcarrier demapping matrix of the *kth* user. $\boldsymbol{W}_{MMSE}{}^{k}$ can be expressed as [15]

$$\boldsymbol{W}_{MMSE}{}^{k} = (\mathbf{\Lambda}^{kH} \mathbf{\Lambda}^{k} + 1/SNR)^{-1} \mathbf{\Lambda}^{kH} \tag{11}$$

One major drawback of the MMSE equalizer is the requirement for estimation of the SNR at the receiver. This can be achieved by transmitting specifically chosen pilot sequences and subsequently measuring the SNR at the receiver.

Finally, the estimated modulated symbols undergo demodulation, decoding, and image decompression processes to obtain the original transmitted image.

2.2 Conventional DFT-OFDMA system

The conventional DFT-OFDMA and DST-OFDMA systems exhibit similar levels of complexity for their respective transmitter schemes. However, at the receiver end, which serves as the base station, the DST-OFDMA system incurs slightly greater complexity than the DFT-OFDMA system. This is because the DST-OFDMA system still relies on the DFT and IDFT for the one-tap frequency domain equalizer. Despite this increase in complexity, the benefits of the DST-OFDMA system make the elevated complexity in the uplink acceptable.

3 Image compression methods

Mostly, image compression methods are used to minimize the image data size while keeping the needed information to recover the compressed image effectively. Compression methods can be divided into two types. Lossless compression is a method of compression that does not result in any loss of information. This type of compression is used when it is important to maintain the quality of the original image, such as in medical imaging, legal images and graphic design applications. Lossless compression works by identifying and eliminating redundant data in the image file. Examples of lossless compression methods include PNG and GIF. Lossy compression, on the other hand,

is a method of compression that results in a loss of some of the original image data. This type of compression is used when a high compression ratio is required, such as in web-based applications or digital photography. Lossy compression works by identifying and removing non-essential data from the image file, such as high-frequency noise or color information that is not perceptible to the human eye. Image compression methods are an important part of modern digital communication and media technologies, allowing for efficient storage and transmission of large amounts of image data. However, it is important to choose the appropriate compression method depending on the specific application and requirements for image quality and file size.

Nine compression methods were taken from the Wavelet Toolbox of MATLAB and used to analyze the performance of compressed-image transmission over DST-OFDMA, see Table 1.

Compression methods aim to improve bandwidth efficiency by reducing the amount of data required for transmission or storage. Techniques like SPIHT, SPIHT-3D, and EZW have shown high compression efficiency, making them popular for bandwidth-limited applications. However, the effectiveness of a method depends on the data characteristics. Evaluating and comparing different methods is crucial to determine the most suitable and bandwidth-efficient option for specific applications. Among the compression methods in Table 1, SPIHT and SPIHT-3D are well-known for their high compression efficiency. They utilize a progressive encoding approach that prioritizes significant coefficients, resulting in high compression ratios.

4 Simulation results and discussion

The simulation results are carried out using MATLAB 2020 to compute and compare the minimum required SNR value to recover the transmitted compressed image over DFT-LOFDMA, DFT-IOFDMA, DST-LOFDMA, and DST-IOFDMA systems. Different compression methods, modulation schemes, and subcarrier mapping schemes are used over vehicular A, SUI3 and Uniform channel models. Three scenarios are considered. The experimental steps are depicted in Fig. 2. The wpeppers.jpg image of MATLAB 2020 is used and shown in Fig. 3. The parameters of OFDMA system are tabulated in Table 2.

Table 1 The used nine compression Methods with their compression MSE and PSNR

No.	Compression method	MSE	PSNR
1	Set partitioning in hierarchical trees (SPIHT): [20, 21]	79.09	29.15
2	Spatial-orientation Tree Wavelet (STW): [20]	47.534	31.361
3	Set Partitioning In Hierarchical Trees 3D for true color images (SPIHT-3D) [22]	57.1024	30.5643
4	Embedded Zerotree Wavelet (EZW) [23]	31.613	33.132
5	wavelet difference Reduction (WDR) [24]	24.471	34.244
6	Adaptively Scanned Wavelet Difference Reduction (ASWDR) [25, 26]	22.2029	34.6667
7	Subband thresholding of coefficients and Huffman encoding (lvl_mmc)	14.638	36.476
8	Global thresholding of coefficients and fixed encoding (GBL_MMC_F) [26, 27]	49.4474	31.1894
9	Global thresholding of coefficients and Huffman encoding (GBL_MMC_H) [26, 27]	49.4801	31.1865

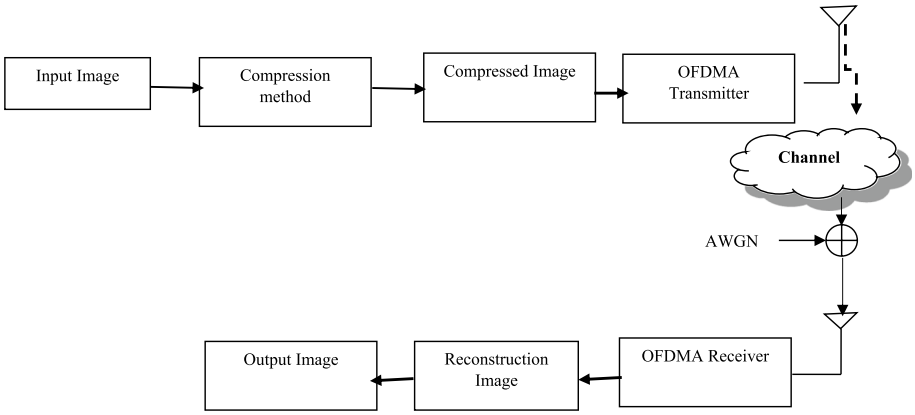

Fig. 2 System model of compressed image transmission over the DST-OFDMA system. The system model for compressed image transmission over the discrete sine transform OFDMA system is illustrated in the figure, which comprises three main parts: the transmitter site, the channel used for transmission, and the receiver site

Fig. 3 The compressed colored wpeppers image with size 512 × 512. Legend: N/A

4.1 The first scenario

In this scenario, the compressed image is transmitted via DFT-LOFDMA, DFT-IOFDMA, DST-LOFDMA and DST-IOFDMA with QPSK and 16QAM modulations over vehicular A channel. The minimum SNR values for recovering the received compressed image using different compression methods are listed in Table 3 and plotted in Fig. 4.

Table 2 Simulation parameters

Parameter	Specification
Simulation method	Monte Carlo
The total number of subcarriers	M = 256
Number of users	4
Modulation Type	QPSK and 16QAM
The channel model used	Vehicular A channel, SUI3, Uniform channel
the channel code	Convolutional code with rate ½
Subcarriers mapping mode	Interleaved and Localized
Cyclic prefix length	20 samples
Channel estimation	Perfect
System bandwidth	5 MHz
Equalization	MMSE

Table 3 The required minimum SNR to recover the transmitted compressed image for the first scenario

Method no.	Compression Method	Vehicular A channel							
		DFT-LOFDMA		DFT-IOFDMA		DST-LOFDMA		DST-IOFDMA	
		QPSK	16QAM	QPSK	16QAM	QPSK	16QAM	QPSK	16QAM
1	SPIHT	40	47	29	41	29	42	24	27
2	STW	39	33	30	39	31	35	24	28
3	STCHE	32	46	32	42	27	45	22	30
4	Ezw	33	51	33	40	25	45	22	32
5	WDR	36	44	30	36	31	42	22	30
6	ASWDR	33	44	30	40	32	45	23	30
7	SPIHT_3D	31	33	23	36	27	32	21	29
8	GBL_MMC_F	34	32	30	37	31	44	25	30
9	GBL_MMC_H	36	33	36	35	34	37	22	35

As shown in Table 3 and Fig. 4, the minimum SNR is about 21 dB which has been achieved by DST-IOFDMA, when the QPSK modulation scheme and SPIHT_3D compression method are used. Moreover, it is generally observed that the DST-OFDMA system has better performance than DFT-OFDMA when QPSK modulation is used.

4.2 The second scenario

In this scenario, the compressed image is transmitted over the SUI3 channel model for DST-LOFDMA, DST-IOFDMA, DFT-LOFDMA and DFT-IOFDMA with QPSK and 16QAM modulations. the required minimum SNR values to recover the transmitted compressed image for the nine compression methods are shown in Fig. 5 and listed in Table 4. It is observed that the minimum SNR is 18 dB which was obtained by DST-IOFDMA with SPIHT_3D compression method. Generally, DST-OFDMA has better performance as compared with DFT-OFDMA system especially with QPSK modulation approach.

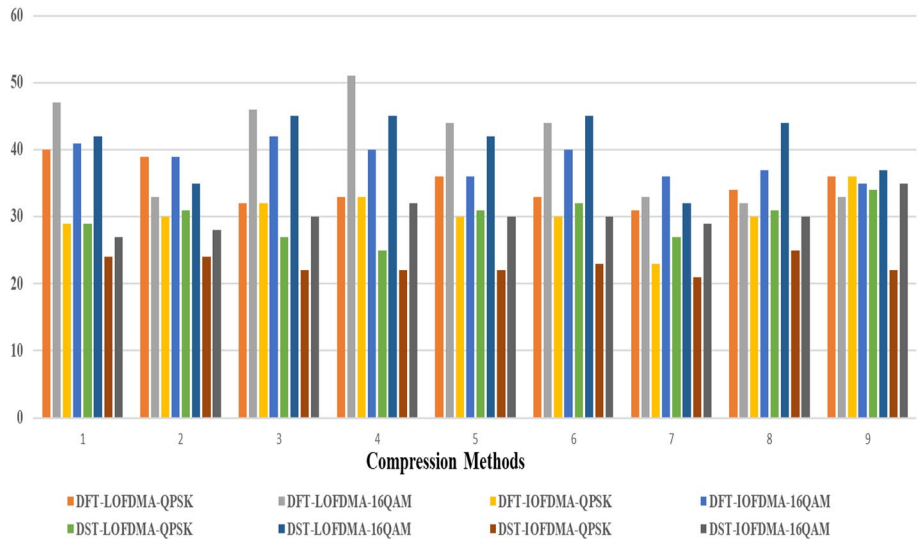

Fig. 4 The minimum SNR to recover the transmitted compressed image over vehicular A channel. The figure shows measurements of SNR on the y-axis for eight different systems, with the x-axis numbered from 1 through 9 to indicate the use of nine compression methods. The measurements were obtained using the Vehicular A channel model

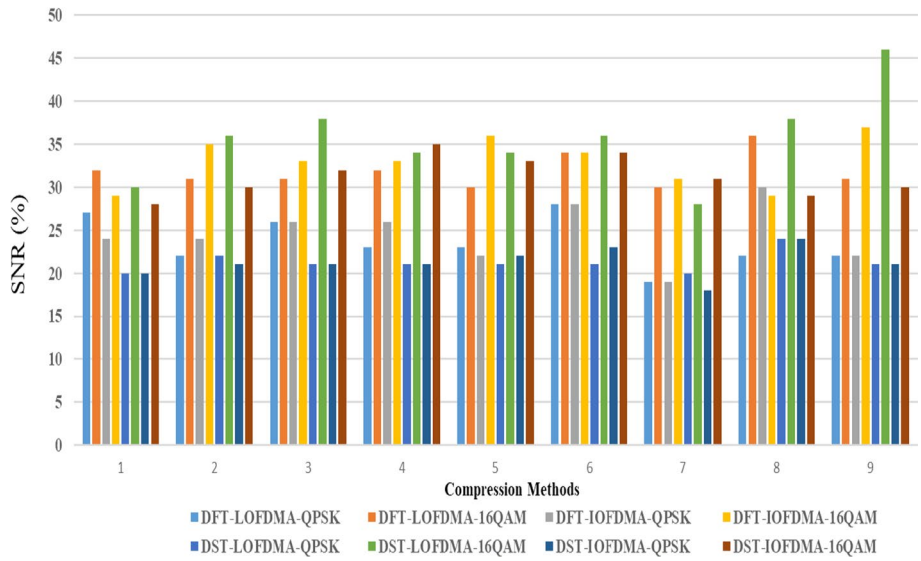

Fig. 5 The minimum SNR to recover the transmitted compressed image over SUI3 channel. Measurements of SNR for eight different systems are presented in the figure, where the y-axis displays the values and the x-axis is numbered from 1 through 9 to represent the use of nine compression methods. The measurements were acquired using the SUI3 channel model

4.3 The third scenario

The third scenario describes the required minimum SNR to recover the transmitted compressed image for DST-LOFDMA, DST-IOFDMA, DFT-LOFDMA and DFT-IOFDMA when Uniform channel is used with QPSK and 16QAM modulation approaches. The obtained results are shown in Table 5 and Fig. 6. It is noted that the

Table 4 The minimum SNR to recover the transmitted compressed image when SUI3 channel

Method no.	Compression method	SUI3 channel							
		DFT-LOFDMA		DFT-IOFDMA		DST-LOFDMA		DST-IOFDMA	
		QPSK	16QAM	QPSK	16QAM	QPSK	16QAM	QPSK	16QAM
1	SPIHT	27	32	24	29	20	30	20	28
2	STW	22	31	24	35	22	36	21	30
3	STCHE	26	31	26	33	21	38	21	32
4	Ezw	23	32	26	33	21	34	21	35
5	WDR	23	30	22	36	21	34	22	33
6	ASWDR	28	34	28	34	21	36	23	34
7	SPIHT_3D	19	30	19	31	20	28	18	31
8	GBL_MMC_F	22	36	30	29	24	38	24	29
9	GBL_MMC_H	22	31	22	37	21	46	21	30

Table 5 The minimum SNR to recover the transmitted compressed image over uniform channel

Method no.	Compression method	Uniform channel							
		DFT-LOFDMA		DFT-IOFDMA		DST-LOFDMA		DST-IOFDMA	
		QPSK	16QAM	QPSK	16QAM	QPSK	16QAM	QPSK	16QAM
1	SPIHT	34	33	25	31	32	39	20	30
2	STW	28	35	25	37	25	35	22	35
3	STCHE	31	45	35	32	30	40	20	31
4	Ezw	26	36	35	42	33	38	23	30
5	WDR	35	45	27	38	26	42	23	32
6	ASWDR	36	38	35	36	30	38	21	33
7	SPIHT_3D	27	35	26	31	26	34	21	29
8	GBL_MMC_F	25	37	35	34	30	36	25	31
9	GBL_MMC_H	27	35	26	34	26	36	21	33

smallest SNR is 20 dB. This value has been obtained by the DST-IOFDMA system when the QPSK modulation approach and SPIHT and STW compression methods are used.

For more clarification, we can compare all the scenarios for all channels based on the type of the modulation schemes as follows. Firstly, as shown in Fig. 7 and Table 6, we compare the SNR values of DST-LOFDMA, DST-IOFDMA, DFT-LOFDMA, and DFT-IOFDMA systems when employing the QPSK modulation scheme. This comparison is performed across the nine compression methods over vehicular A, SUI3, and Uniform channels. Figure 7 and Table 6 show that the smallest SNR is 18 dB which was achieved by DST-IOFDMA system for SPIHT_3D compression method.

Secondly, Fig. 8 and Table 7 present a comparison of the SNR values for DST-LOFDMA, DST-IOFDMA, DFT-LOFDMA, and DFT-IOFDMA systems when utilizing the 16QAM modulation scheme. This evaluation encompasses the nine compression methods across vehicular A, SUI3, and Uniform channels. Figure 8 and Table 7 show

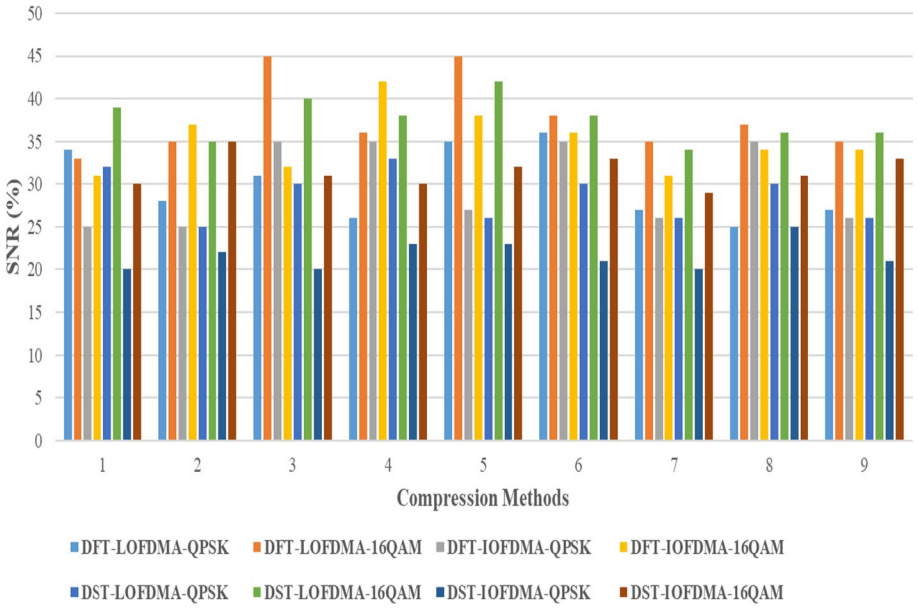

Fig. 6 The minimum SNR to recover the transmitted compressed image when Unform channel is used. Displayed in the figure are measurements of SNR for eight different systems, where the y-axis denotes the values and the x-axis is numbered from 1 through 9 to signify the use of nine compression methods. The measurements were collected using the Uniform channel model

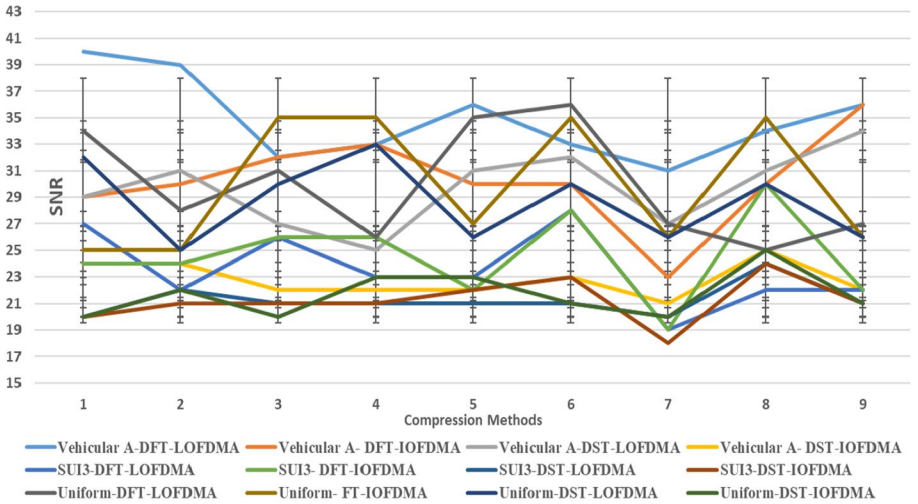

Fig. 7 SNR of The Systems for nine compression methods, QPSK over Vehicular, SUI3 and Unform channels. The figure illustrates the evaluation of the minimum SNR of the systems for the QPSK modulation scheme over Vehicular, SUI3, and Uniform channels, considering nine compression methods

that the smallest SNR is 27 dB which was achieved by DST-IOFDMA system for SPIHT compression method.

Lastly, Table 8 shows the minimum required SNR for each compression method with the suitable systems. It is concluded that the appropriate system for compressed-image transmission is DST-OFDMA with QPSK modulation and SUI3 channel model as compared with DFT-OFDMA.

Table 6 SNR of the systems for nine compression methods, QPSK over Vehicular A, SUI3 and uniform channels

Method no.	Vehicular A-DFT-LOFDMA	Vehicular A-DFT-IOFDMA	Vehicular A-DST-LOFDMA	Vehicular A-DST-IOFDMA	SUI3-DFT-LOFDMA	SUI3-DFT-IOFDMA	SUI3-DST-LOFDMA	SUI3-DST-IOFDMA	Uniform-DFT-LOFDMA	Uniform-FT-IOFDMA	Uniform-DST-LOFDMA	Uniform-DST-IOFDMA
1	40	29	29	24	27	24	20	20	34	25	32	20
2	39	30	31	24	22	24	22	21	28	25	25	22
3	32	32	27	22	26	26	21	21	31	35	30	20
4	33	33	25	22	23	26	21	21	26	35	33	23
5	36	30	31	22	23	22	21	22	35	27	26	23
6	33	30	32	23	28	28	21	23	36	35	30	21
7	31	23	27	21	19	19	20	18	27	26	26	20
8	34	30	31	25	22	30	24	24	25	35	30	25
9	36	36	34	22	22	22	21	21	27	26	26	21

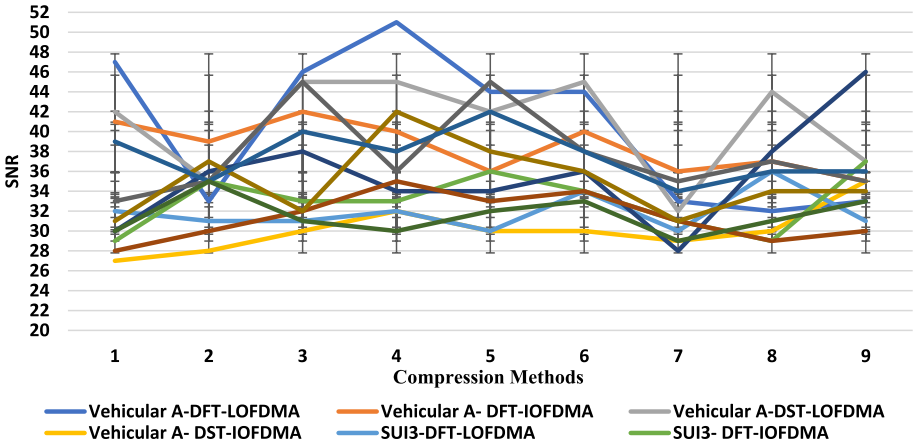

Fig. 8 SNR of the Systems for the nine compression techniques, 16QAM over Vehicular, SUI3 and Uniform channels. The figure provides a visual representation of the analysis conducted to determine the minimum SNR of the systems using 16QAM modulation scheme over Vehicular, SUI3, and Uniform channels, with a consideration of nine compression methods

5 Conclusion

In this paper, the transmitted compressed image via the DST-OFDMA system has been analyzed and compared with the DFT-OFDMA system using several compression methods when different channel models, different modulation schemes, and different subcarrier mapping schemes were used. The minimum required SNR to recover the compressed image was computed for three scenarios as follows. In the first scenario, the transmission of a compressed image over DST-IOFDMA, DST-LOFDMA, DFT-IOFDMA and DFT-LOFDMA systems were studied when vehicular A channel, QPSK and 16QAM modulation schemes were used. In the second and the third scenarios, the same evaluation was applied but over SUI3 and Uniform channel models, respectively. The simulation results were carried out using MATLAB 2020 and shown that the smallest value of SNR was 18 dB to recover the compressed transmitted image. This value was obtained when the DST-IOFDMA system was used with the SPIHT_3D compression method and QPSK modulation over the SUI3 channel model. This indicated that SPIHT_3D has lower power consumption as compared with other compression methods in addition to its high bandwidth efficiency. Furthermore, the obtained results have shown that the performance of DST-OFDMA is better than DFT-OFDMA, especially when QPSK modulation was used over the SUI3 channel model. For future work, it would be interesting to study impact of the carrier frequency offsets as well as the imperfect channel estimation on the transmission of compressed image over DFT-OFDMA and DST-OFDMA. Moreover, it is also interesting to expand this research to include more advanced modulation and coding systems for MIMO system, operating in the millimeter wave frequency band like 5G networks.

Table 7 SNR of The Systems for nine compression methods, 16QAM over Vehicular, SUI3 and Uniform channels

Method no.	Vehicular A-DFT-LOFDMA	Vehicular A-DFT-IOFDMA	Vehicular A-DST-LOFDMA	Vehicular A-DST-IOFDMA	SUI3-DFT-LOFDMA	SUI3-DFT-IOFDMA	SUI3-DST-LOFDMA	SUI3-DST-IOFDMA	Uniform-DFT-LOFDMA	Uniform-DFT-IOFDMA	Uniform-DST-LOFDMA	Uniform-DST-IOFDMA
1	47	41	42	27	32	29	30	28	33	31	39	30
2	33	39	35	28	31	35	36	30	35	37	35	35
3	46	42	45	30	31	33	38	32	45	32	40	31
4	51	40	45	32	32	33	34	35	36	42	38	30
5	44	36	42	30	30	36	34	33	45	38	42	32
6	44	40	45	30	34	34	36	34	38	36	38	33
7	33	36	32	29	30	31	28	31	35	31	34	29
8	32	37	44	30	36	29	38	29	37	34	36	31
9	33	35	37	35	31	37	46	30	35	34	36	33

Table 8 Appropriate compression method(s) for appropriate OFDMA system (s)

No.	Appropriate compress method	Minimum SNR (dB) ≥	Appropriate system (s)
1	SPIHT	20	DST-LOFDMA-QPSK-SUI3, DST-IOFDMA-QPSK-SUI3, DST-IOFDMA-QPSK-Uniform
2	STW	21	DST-IOFDMA-QPSK-SUI3
3	STCHE	21	DST-IOFDMA-QPSK- Uniform
4	Ezw	21	DST-LOFDMA-QPSK-SUI3, DST-IOFDMA-QPSK-SUI3
5	WDR	21	DST-LOFDMA-QPSK- SUI3
6	ASWDR	21	DST-LOFDMA-QPSK-SUI3 DST-IOFDMA-QPSK-Uniform
7	SPIHT_3D	18	DST-IOFDMA-QPSK-SUI3
8	GBL_MMC_F	22	DFT-LOFDMA-QPSK-SUI3
9	GBL_MMC_H	21	DST-LOFDMA-QPSK-SUI3, DST-IOFDMA-QPSK-SUI3 DST-IOFDMA-QPSK-Uniform

Abbreviations

DST	Discrete Sine transform
DFT	Discrete Fourier transform
LOFDMA	Localized OFDMA
IDST	Inverse DST
IOFDMA	Interleaved OFDMA
SPIHT	Set partitioning in hierarchical trees
STW	Spatial-orientation tree wavelet
SPIHT-3D	Set partitioning in hierarchical trees 3D for true color images
EZW	Embedded Zerotree Wavelet
WDR	Wavelet difference Reduction
ASWDR	Adaptively scanned wavelet difference reduction
lvl_mmc	Subband thresholding of coefficients and Huffman encoding
GBL_MMC_F	Global thresholding of coefficients and fixed encoding
GBL_MMC_H	Global thresholding of coefficients and Huffman encoding
SNR	Signal-to-noise ratio
MSE	Mean square error
PSNR	Peak signal-to-noise ratio

Author contributions

N.H and K.A.M. contributed to writing—original draft, data curation, visualization, analyzing the collected articles. M.A.S.contributed to conceptualization, supervision, project administration, review. F.S. helped in writing, editing, review. All the authors contributed to the general discussion and revision of the manuscript.

Availability of data materials

The data in this study are available from the corresponding author upon request.

Declarations

Competing interests

The authors declare no competing interests.

Received: 14 March 2023 Accepted: 7 August 2023
Published online: 16 August 2023

References

1. S.N. Dessai, H. Patidar, Software design analysis and implementation of OFDMA and its computing architecture analysis for 5G/4G eNodeB. Wirel. Pers. Commun. **130**, 1371–1397 (2023). https://doi.org/10.1007/s11277-023-10335-1
2. M.M. da Silva, J. Guerreiro, On the 5G and beyond. Appl. Sci. **10**(20), 7091 (2020). https://doi.org/10.3390/app10207091
3. F.S. Al-Kamali, A.F. Al-Junaid, M.Y. Al-Shamri, New image transmission schemes for DST-based MC-CDMA system. Arab. J. Sci. Eng. **46**(2), 1465–1479 (2021)

4. F.S. Al-kamali, F.A. Al-Fuhaidy, K.A. Al-soufy, Wireless image transmissions over frequency selective channel using recent OFDMA systems. Am. J. Comput. Commun. Control **5**(1), 30–38 (2018)
5. E. Mehallel, D. Abed, A. Boukaache, A. Bouchemel, Enhancement of image transmission using chaotic interleaving with discrete wavelet transform-based single-carrier frequency division multiple access system. Int. J. Commun. Syst. **34**(7), e4728 (2021)
6. P. Hazowary, S.K. Dutta, R. Subadar, *A comparison of image compression techniques over wireless fading channel. Contemporary issues in communication, cloud and big data analytics* (Springer, Singapore, 2022), pp.241–249
7. P. S., Babu, S. Sathappan: Effective compressed image transmission through context aware wireless networks. In: 2016 IEEE International Conference on Advances in Computer Applications (ICACA), pp. 82–86. IEEE (2016)
8. H. Kasban, S. Nassar, M.A.M. El-Bendary, Medical images transmission over wireless multimedia sensor networks with high data rate. Analog Integr. Circuits Signal Process. **108**(1), 125–140 (2021)
9. O. Ghorbel, W. Ayedi, M. W. Jmal, and M. Abid, Images compression in WSN: Performance analysis, in 2012 IEEE 14th International Conference on Communication Technology, pp. 1363–1368 (2012)
10. D. M. Pham and S. M. Aziz, FPGA-based image processor architecture for wireless multimedia sensor network, in 2011 IFIP 9th International Conference on Embedded and Ubiquitous Computing, pp. 100–105 (2011)
11. H. Zain Eldin, M.A. Elhosseini, H.A. Ali, Image compression algorithms in wireless multimedia sensor networks: a survey. Ain Shams Eng. J. **6**(2), 481–490 (2015)
12. T. Kawai, Video slice: image compression and transmission for agricultural systems. Sensors **21**(11), 3698 (2021)
13. N.H. Al-Ashwal, K.A. Al-Soufy, F.S. Al-Kamali, M.A. Swillam, Performance evaluation of wireless compressed-image transmission over discrete Fourier transform-based orthogonal frequency division multiple access system. J. Eng. **2022**(6), 656–664 (2022)
14. F.A.K. Al-Fuhaidy, K.A. Al-Sofy, F.S. Alkamali, Discrete sine transform based OFDMA system for wireless broadband communications
15. F.E. Abd El-Samie, F.S. Al-Kamali, A.Y. Al-Nahari, M.I. Dessouky, *SC-FDMA for Mobile Communications* (CRC Press, Boca Raton, 2013)
16. Z. Lin et al., Refracting RIS aided hybrid satellite-terrestrial relay networks: Joint beamforming design and optimization. IEEE Trans. Aerosp. Electron. Syst. **58**(4), 3717–3724 (2022)
17. Z. Lin, M. Lin, T. de Cola, J.-B. Wang, W.-P. Zhu, J. Cheng, Supporting IoT with rate-splitting multiple access in satellite and aerial-integrated networks. IEEE Internet Things J. **8**(14), 11123–11134 (2021)
18. Z. Lin et al., SLNR-based secure energy efficient beamforming in multibeam satellite systems. IEEE Trans. Aerosp. Electron. Syst. **59**(2), 2085–2088 (2023)
19. M. Alouzi, F. Al-Kamali, C. D'Amours, F. Chan, Direct conversion of hybrid precoding and combining from full array architecture to subarray architecture for mmWave MIMO systems. IEEE Access J. **11**, 35457–35468 (2023)
20. A. Said, W.A. Pearlman, A new, fast, and efficient image codec based on set partitioning in hierarchical trees. IEEE Trans. Circuits Syst. Video Technol. **6**(3), 243–250 (1996)
21. M.A. Kabir, M.A.M. Khan, M.T. Islam, M.L. Hossain, A.F. Mitul, Image compression using lifting based wavelet transform coupled with SPIHT algorithm, in 2013 International Conference on Informatics, Electronics and Vision (ICIEV), pp. 1–4 (2013)
22. B.-J. Kim, W.A. Pearlman, An embedded wavelet video coder using three-dimensional set partitioning in hierarchical trees (SPIHT), in Proceedings DCC '97. Data Compression Conference, pp. 251–260 (2002)
23. J.M. Shapiro, Embedded image coding using zero trees of wavelet coefficients. IEEE Trans. Signal Process. **41**(12), 3445–3462 (1993)
24. Y. Yuan, M.K. Mandal, Novel embedded image coding algorithms based on wavelet difference reduction. IEE Proc. Vis. Image Signal Process. **152**(1), 9 (2005)
25. J.S. Walker, Lossy image codec based on adaptively scanned wavelet difference reduction. Opt. Eng. **39**(7), 1891 (2000)
26. O.S. Devi, H. Kumar, S.B. Patil, Compression and decompression of time series signals using two wavelet coefficients thresholding techniques and their comparisons. IJOAR, 1–8, (2013)
27. R. Kumar, S. Singh, Comparative analysis of wavelet based compression methods. Int. J. Comput. Netw. Wirel. Mobile Commun. **4**(2), 143–150 (2014)

Publisher's Note